Branch-entangled polariton pairs in planar microcavities and photonic wires

C. Ciuti
Laboratoire Pierre Aigrain, Ecole Normale Supérieure, 24, rue Lhomond, 75005 Paris, France
(Received 17 December 2003; published 9 June 2004)

A scheme is proposed for the generation of branch-entangled pairs of microcavity polaritons through spontaneous interbranch parametric scattering. Branch entanglement is achievable when there are two twin processes, where the role of signal and idler can be exchanged between two different polariton branches. Branch entanglement of polariton pairs can lead to the emission of frequency-entangled photon pairs out of the microcavity. In planar microcavities, the necessary phase-matching conditions are fulfilled for pumping of the upper polariton branch at an arbitrary in-plane wave vector. The important role of nonlinear losses due to pair scattering into high-momentum exciton states is evaluated. The results show that the lack of protection of the pump polaritons in the upper branch is critical. In photonic wires, branch entanglement of one-dimensional polaritons is achievable when the pump excites a lower polariton sub-branch at normal incidence, providing protection from the exciton reservoir.

DOI: 10.1103/PhysRevB.69.245304 PACS number(s): 71.36.+c

INTRODUCTION

The generation of entangled states is one of the most fascinating aspects of quantum mechanics.[1] In quantum optics, parametric sources of entangled photon pairs have been attracting great interest due to their remarkable nonclassical applications. In particular, polarization-entangled pairs of photons[2] are an essential ingredient for quantum cryptography,[3] while frequency-entangled pairs have been recently exploited for the so-called quantum optical coherence tomography.[4] In atomic physics, parametric collisions are also enjoying considerable attention with the possibility of creating entangled pairs of atoms by parametric scattering off a Bose-Einstein condensate.[5]

Recently, semiconductor quantum microcavities in the strong exciton-photon coupling regime[6,7] have been shown to provide very rich parametric phenomena.[8–16] In these systems, the strong coupling between quantum well exciton and cavity photon modes gives rise to two branches of quasi-two-dimensional bosons, the so-called lower and upper branch polaritons. In a polariton device, the parametric scattering is due to polariton-polariton interactions, which are extremely efficient.[9,14] Moreover, the energy-momentum conservation (phase matching) can be provided intrinsically by the peculiar shape of the polariton energy dispersion. Interestingly, semiconductor planar microcavities can be laterally patterned with the possibility of creating zero-dimensional[17] and one-dimensional[18] (1D) polariton systems with controllable parametric properties. Efficient interbranch parametric scattering has been demonstrated in one-dimensional microcavities,[18] where the presence of several polariton sub-branches provides the opportunity of tailoring the parametric processes in a remarkable way.

While the outstanding optical gain properties of polariton parametric amplifiers involving the lower branch are largely investigated, the study of the genuine quantum properties is still in its infancy. So far, current research has been focused on the generation and detection of polariton squeezing[19] due to the anomalous correlation between signal and idler polaritons, both belonging to the lower branch. Polariton squeezing has been recently demonstrated in the degenerate configuration[13,20] (signal, pump, and idler in the same lower polariton branch mode), but the detection of two-mode squeezing in the nondegenerate configuration appears challenging due to the very different extra-cavity radiative coupling of signal and idler modes within the lower branch.[21]

One important issue yet to be explored is the possibility of creating Einstein-Podolski-Rosen (EPR) pairs of polaritons, which are entangled with respect to a certain degree of freedom and which can be efficiently transferred out of the microcavity. In this paper, we propose a scheme to create polariton pairs, which are entangled with respect to a peculiar degree of freedom, namely, the discrete polariton branch index. We show that spontaneous interbranch parametric scattering can generate pairs in the entangled state of the form

$$|\Psi\rangle \propto |j_1,k_s\rangle|j_2,k_i\rangle + |j_2,k_s\rangle|j_1,k_i\rangle, \tag{1}$$

where $|j,k\rangle$ denotes a polariton state belonging to the jth branch (or sub-branch) mode with wave vector k. The signal and idler wave vectors (k_s and k_i) are such to provide phase matching for the two branch-exchanged processes, as it will be discussed later in detail. We show that the necessary (but not sufficient) phase-matching requirements for this kind of parametric effect are easily fulfilled both in two-dimensional systems (planar microcavities) and one-dimensional structures (photonic wires), thanks to the dispersion of polariton branches, which can be engineered. In our study, we evaluate the protection of the considered parametric process from nonlinear losses (collision broadening). In planar microcavities, we find that pair scattering into the exciton reservoir can be a severe limitation. In fact, when the pump drives the upper branch, pump-pump, pump-signal, and pump-idler scattering into the high-momentum exciton states is particularly efficient. In photonic wires, this lack of protection of pump polaritons in the upper branch can be naturally defeated. In fact, in photonic wires, the additional confinement of the photon modes produces a many-fold of sub-branches. In these systems, interbranch scattering is possible even under pump excitation of the lower sub-branch, as recently demonstrated experimentally.[18] We show that by pumping a lower sub-branch at normal incidence ($k_x=0$), branch-

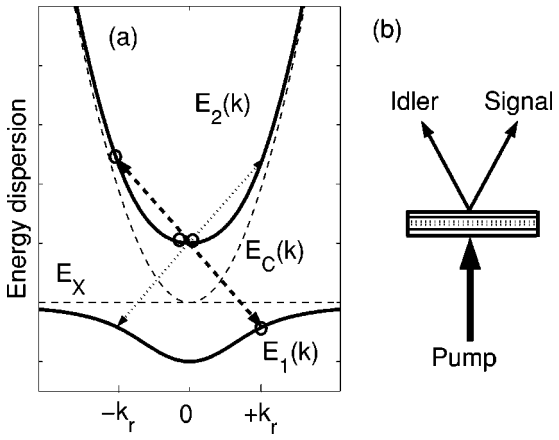

FIG. 1. (a) Solid lines: in-plane energy dispersion $E_1(k)[E_2(k)]$ for the lower (upper) polariton branch. Dashed lines: dispersion $E_C(k)[E_X(k)]$ of the cavity (exciton) mode. Arrows depict the considered interbranch polariton pair scattering process. (b) Sketch of the excitation geometry of the planar microcavity.

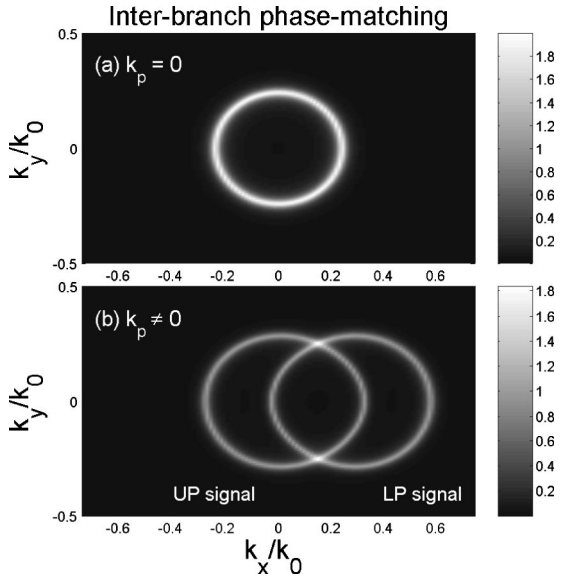

FIG. 2. Phase-matching function $\eta(\mathbf{k})$ (defined in the text) as a function of the signal in-plane wave vector $\mathbf{k}$ (k_0 units). (a) The pump excites the upper branch at normal incidence ($\mathbf{k}_p=\mathbf{0}$). (b) $\mathbf{k}_p=0.15\ k_0\hat{\mathbf{x}}$. Parameters: $E_X=E_C(0)=1.5\ eV$, $k_0=E_C(0)/(\hbar c)$, $2\hbar\Omega_R=4$ meV, $\gamma=0.5$ meV.

entangled pairs of polaritons with a finite wave vector can be obtained. Since the pumped mode lies in a lower sub-branch, pump-pump, pump-signal, and pump-idler scattering into the exciton reservoir can be suppressed.

The paper is organized as follows. In Sec. I A, we describe the proposed interbranch process in a planar microcavity, where the upper polariton branch is excited. The generation of branch-entangled pairs of polaritons is treated within a quantum Hamiltonian model, presented in Sec. I B. Section I C treats the coupling to the extra-cavity field, which is responsible for the spontaneous emission of frequency-entangled pairs of photons. In Sec. I D and I E, we address the important issue of nonlinear losses. In Sec. II, we consider the case of photonic wires. Finally, conclusions are drawn in Sec. III.

I. 2D MICROCAVITIES

A. Phase matching for interbranch scattering

We start by giving the general idea of the proposed process and then we turn to a more detailed theoretical analysis. The strong coupling between exciton and cavity photon modes is known to produce an anticrossing of their energy dispersions $E_C(k)$ and $E_X(k)$, resulting in the appearance of the lower and upper polariton branches, whose energy dispersions $E_1(k)$ and $E_2(k)$ are depicted in Fig. 1(a). So far, studies of polariton parametric scattering in planar microcavities have focused on the lower branch, in particular, under pump excitation near the inflection point of the lower branch dispersion. Here, we consider a different process, which involves both branches. Suppose a pump laser injects polaritons in the upper branch state with zero in-plane wave vector ($\mathbf{k}_p=\mathbf{0}$). Two injected upper polaritons can scatter coherently, being parametrically converted into a signal-idler pair of polaritons, namely, a lower and an upper polariton with opposite in-plane momentum [see Figs. 1(a) and 1(b)]. The phase matching is fulfilled when the idler and signal wave vector are such that $|\mathbf{k}_s|=|\mathbf{k}_i|=k_r$, where k_r depends on the polariton splitting and exciton-photon detuning. Note that for a given $\mathbf{k}_s$, there are two equivalent processes, where the role of signal and idler is exchanged between the lower and upper polariton branch. Quantum entanglement is due to our ignorance on which of the two scattered polaritons is in the lower or upper branch. Figure 2 depicts the phase-matching pattern in the two-dimensional momentum space. We have plotted the phase-matching function $\eta(\mathbf{k})=\eta_1(\mathbf{k})+\eta_2(\mathbf{k})$, with

$$\eta_{1(2)}(\mathbf{k})=\frac{\gamma^2}{[E_{1(2)}(\mathbf{k})+E_{2(1)}(2\mathbf{k_p}-\mathbf{k})-2E_2(\mathbf{k_p})]^2+\gamma^2}, \tag{2}$$

where γ represents the polariton broadening. Note that if the energy-momentum conservation for the interbranch scattering is strongly violated, $\eta_{1(2)}(\mathbf{k})\to 0$. On the other hand, when $\mathbf{k}$ is an exact phase-matching wave vector for a lower (upper) polariton signal, $\eta_{1(2)}(\mathbf{k})=1$. Importantly, if a wave vector $\mathbf{k}$ is phase matching for both branches, then $\eta(\mathbf{k})=2$. Figure 2(a) shows the case $\mathbf{k_p}=\mathbf{0}$, where $\eta_1(\mathbf{k})=\eta_2(\mathbf{k})$ and $\eta(\mathbf{k})=2$ on the ring $|\mathbf{k}|=k_r$. Entangled polariton pairs can be achieved with opposite momentum on the ring. On the other hand, Fig. 2(b) shows the case $\mathbf{k_p}\neq\mathbf{0}$, where the lower and upper branch signal phase-matching curves split [$\eta_1(\mathbf{k})\neq\eta_2(\mathbf{k})$] and branch entanglement is possible only at the two intersection points. Note that this phase-matching profile is topologically different from the ∞-shaped profile obtained under pumping of the lower branch.[22,23] Moreover, we point out that the pattern in Fig. 2(b) is reminiscent of the one achieved in type-II parametric down-conversion, which generates polarization-entanglement of photon pairs.[2]

B. Quantum Hamiltonian description

We now turn to a detailed treatment of this system. As a result of the strong exciton-photon coupling, the lower and upper polariton boson operators $p_{1,\mathbf{k}}$ and $p_{2,\mathbf{k}}$ are linked to the quantum well exciton and cavity operators $b_{\mathbf{k}}$ and $a_{\mathbf{k}}$ by an unitary Hopfield transformation, namely,

$$\begin{pmatrix} b_{\mathbf{k}} \\ a_{\mathbf{k}} \end{pmatrix} = \begin{pmatrix} M_{1,1,\mathbf{k}} & M_{1,2,\mathbf{k}} \\ M_{2,1,\mathbf{k}} & M_{2,2,\mathbf{k}} \end{pmatrix} \begin{pmatrix} p_{1,\mathbf{k}} \\ p_{2,\mathbf{k}} \end{pmatrix}. \tag{3}$$

The matrix of Hopfield coefficients $M_{i,j,\mathbf{k}}$ is such that $M_{1,1,\mathbf{k}}=M_{2,2,\mathbf{k}}=1/\sqrt{1+\rho_k^2}$ and $M_{1,2,\mathbf{k}}=-M_{2,1,\mathbf{k}}=\sqrt{1-M_{1,1,\mathbf{k}}^2}$, where $\rho_k=\hbar\Omega_R/[E_1(k)-E_C(k)]$ and $2\hbar\Omega_R$ is the polariton splitting when exciton and photon modes are exactly resonant. Polaritons are interacting bosons, due to the exciton-exciton exchange interaction and due to the anharmonic part of the exciton-photon interaction (saturation),[24,25] whose respective Hamiltonian contributions H_{XX} and H_{XC}^{sat} are

$$H_{XX} = \frac{1}{2}\sum \frac{\lambda_x^2}{A}\frac{6e^2}{\epsilon\lambda_x} b_{\mathbf{k}+\mathbf{q}}^\dagger b_{\mathbf{k}'-\mathbf{q}}^\dagger b_{\mathbf{k}} b_{\mathbf{k}'}, \tag{4}$$

$$H_{XC}^{sat} = -\sum \frac{\hbar\Omega_R}{n_{sat}A}\, a_{\mathbf{k}+\mathbf{q}}^\dagger b_{\mathbf{k}'-\mathbf{q}}^\dagger b_{\mathbf{k}} b_{\mathbf{k}'} + \text{H.c.}, \tag{5}$$

being A the excitation area, λ_X the 2D exciton radius, ϵ the static dielectric constant of the semiconductor and $n_{sat}=7/(16\pi\lambda_X^2)$ the exciton saturation density. In the polariton basis, both effects contribute to create an effective pair interaction potential. In our previous treatment of polariton parametric scattering,[22,25] we limited our description to the lower branch. Including also the upper branch, we get the following effective Hamiltonian describing polariton-polariton interactions:

$$H_{PP} = \frac{1}{2}\sum \frac{\lambda_x^2}{A} V_{\mathbf{k},\mathbf{k}',\mathbf{q}}^{j_1,j_2,j_3,j_4} p_{j_1,\mathbf{k}+\mathbf{q}}^\dagger p_{j_2,\mathbf{k}'-\mathbf{q}}^\dagger p_{j_3,\mathbf{k}} p_{j_4,\mathbf{k}'}, \tag{6}$$

where the effective branch-dependent potential is

$$\begin{aligned} V_{\mathbf{k},\mathbf{k}',\mathbf{q}}^{j_1,j_2,j_3,j_4} = \Bigg\{ & \frac{6e^2}{\epsilon\lambda_x} M_{1,j_1,\mathbf{k}+\mathbf{q}} M_{1,j_2,\mathbf{k}'-\mathbf{q}} M_{1,j_3,\mathbf{k}} M_{1,j_4,\mathbf{k}'} \\ & - \frac{2\hbar\Omega_R}{n_{sat}\lambda_X^2} M_{2,j_1,\mathbf{k}+\mathbf{q}} M_{1,j_2,\mathbf{k}'-\mathbf{q}} M_{1,j_3,\mathbf{k}} M_{1,j_4,\mathbf{k}'} \\ & - \frac{2\hbar\Omega_R}{n_{sat}\lambda_X^2} M_{2,j_4,\mathbf{k}'} M_{1,j_3,\mathbf{k}} M_{1,j_2,\mathbf{k}'-\mathbf{q}} M_{1,j_1,\mathbf{k}+\mathbf{q}} \Bigg\}. \end{aligned} \tag{7}$$

Note that this Hamiltonian is for cocircularly polarized polariton states. The first contribution to $V_{\mathbf{k}',\mathbf{k}',\mathbf{q}}^{j_1,j_2,j_3,j_4}$ is proportional to the 2D exciton binding energy $E_b=e^2/(2\epsilon\lambda_x)$ and is due to the exciton-exciton interaction. This contribution is always repulsive, because $M_{1,j,\mathbf{k}}$ is always positive. The other contribution is due to the anharmonic exciton-photon coupling and can be either positive or negative, depending on the branch indexes.

The regime of polariton parametric scattering takes place when a pump laser drives coherently a single branch at a given wave vector. In this case, the corresponding quantum destruction operator $p_{j_p,\mathbf{k_p}}$ can be approximated by the its mean-field value $\langle p_{j_p,\mathbf{k_p}}\rangle$, which is a classical field. Hence, the pair interaction Hamiltonian H_{PP} can be approximated by the parametric Hamiltonian

$$H_{\text{par}} = \sum_{j_1,j_2}\sum_{\mathbf{k}} E_{\mathbf{k},\mathbf{k_p}}^{j_1,j_2,j_p} \mathcal{P}_{j_p,\mathbf{k_p}}^2 p_{j_1,\mathbf{k}}^\dagger p_{j_2,2\mathbf{k_p}-\mathbf{k}}^\dagger + \text{H.c.}, \tag{8}$$

with

$$E_{\mathbf{k},\mathbf{k_p}}^{j_1,j_2,j_p} = (V_{\mathbf{k_p},\mathbf{k_p},\mathbf{k}-\mathbf{k_p}}^{j_1,j_2,j_p,j_p} + V_{\mathbf{k_p},\mathbf{k_p},\mathbf{k}-\mathbf{k_p}}^{j_2,j_1,j_p,j_p})/2. \tag{9}$$

The dimensionless pump polariton density is defined as $|\mathcal{P}_{j_p,\mathbf{k_p}}|^2=|\langle p_{j_p,\mathbf{k_p}}\rangle|^2\lambda_X^2/A$. The other effect is a mean-field shift of the branch-dependent energy, namely, $\tilde{E}_j(\mathbf{k})=E_j(k)+\Lambda_{\mathbf{k},\mathbf{k_p}}^{j,j_p}|\mathcal{P}_{j_p,\mathbf{k_p}}|^2$, where $\Lambda_{\mathbf{k},\mathbf{k_p}}^{j,j_p}=(V_{\mathbf{k},\mathbf{k_p},\mathbf{0}}^{j,j_p,j,j_p}+V_{\mathbf{k_p},\mathbf{k},\mathbf{0}}^{j_p,j,j_p,j}+V_{\mathbf{k},\mathbf{k_p},\mathbf{k_p}-\mathbf{k}}^{j,j_p,j,j_p}+V_{\mathbf{k_p},\mathbf{k},\mathbf{k}-\mathbf{k_p}}^{j_p,j,j_p,j})/2$.

In this section, we are interested in the case of pump excitation of the upper branch ($j_p=2$), with the final states belonging to two different branches ($j_1\neq j_2$). Since $E_{\mathbf{k},\mathbf{k_p}}^{1,2,2}=E_{\mathbf{k},\mathbf{k_p}}^{2,1,2}$, the parametric interaction Hamiltonian reads

$$H_{\text{par}} = \sum_{\mathbf{k}} E_{\mathbf{k},\mathbf{k_p}}^{1,2,2} \mathcal{P}_{2,\mathbf{k_p}}^2 (p_{1,\mathbf{k}}^\dagger p_{2,2\mathbf{k_p}-\mathbf{k}}^\dagger + p_{2,\mathbf{k}}^\dagger p_{1,2\mathbf{k_p}-\mathbf{k}}^\dagger) + \text{H.c.} \tag{10}$$

When applied on the vacuum state $|0\rangle$, H_{par} generate pairs of polaritons with total in-plane momentum $2\mathbf{k_p}$, which are entangled with respect to the branch index. Indeed, Eq. (10) has the paradigmatic form of Hamiltonian, describing the generation of EPR pairs of bosons, which are entangled with respect to a discrete degree of freedom. In quantum optics, the literature about the nonclassical photon properties associated to this Hamiltonian is impressive.[26] In our case, entanglement concerns polaritonic particles and one peculiar polaritonic degree of freedom, namely, the branch index. The generation of branch-entangled pairs is allowed only when there is phase matching for the two branch-exchanged processes, i.e., $E_1(\mathbf{k})+E_2(2\mathbf{k_p}-\mathbf{k})=2E_2(\mathbf{k_p})$ and $E_2(\mathbf{k})+E_1(2\mathbf{k_p}-\mathbf{k})=2E_2(\mathbf{k_p})$. For $\mathbf{k_p}\neq\mathbf{0}$, there are only two possible signal and idler wave vectors, which are the intersection points in Fig. 2(b), as anticipated. When $\mathbf{k_p}=\mathbf{0}$, branch entanglement is achievable for every pair of in-plane wave vectors ($\mathbf{k}$, $-\mathbf{k}$) on the phase-matching ring $|\mathbf{k}|=k_r$. Figure 3 shows the contours of the interaction energy $E_{\mathbf{k}_r,0}^{1,2,2}$ (units of the exciton binding energy E_b), as a function of the polariton splitting to binding energy ratio $2\hbar\Omega_R/E_b$ and of the normalized detuning $\delta=[E_C(0)-E_X]/(2\hbar\Omega_R)$. As anticipated, Fig. 3 shows that the effective interaction can be either positive or negative (the change of sign occurs across the white-dashed line). The effective interaction is positive when it is dominated by the exciton-exciton interaction, negative when the anharmonic exciton-photon coupling takes over.

C. Emission of frequency-entangled photon pairs

The intracavity polariton parametric scattering dynamics is coupled to the extra-cavity field, giving rise to parametric

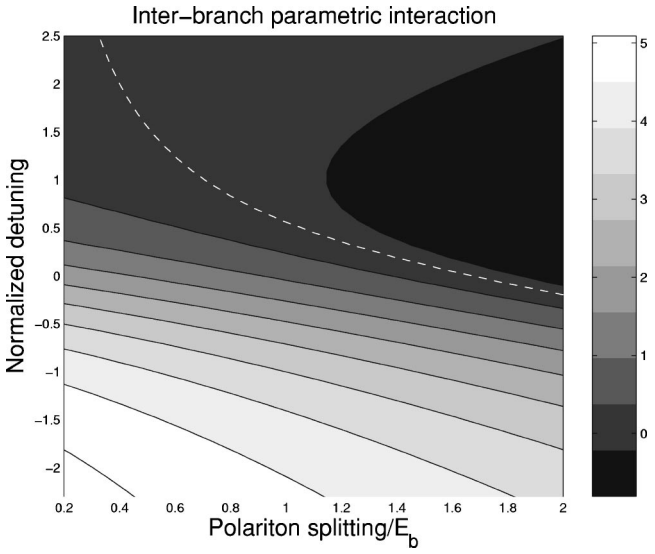

FIG. 3. (a) Contours of the dimensionless parametric interaction energy $E^{1,2,2}_{k_r,0}/E_b$ vs $2\hbar\Omega_R/E_b$ and the normalized detuning $\delta = +[E_C(0)-E_X]/(2\hbar\Omega_R)$. Parameters: $E_C(0)=1.5$ eV, exciton binding energy $E_b=10$ meV. The white-dashed line depicts the zero value points.

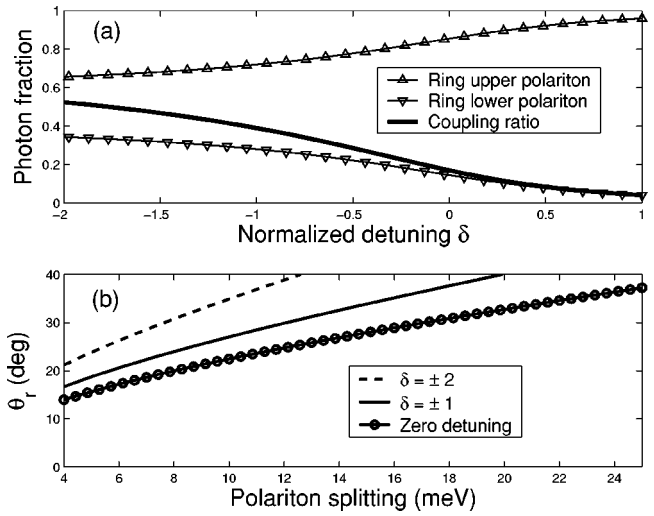

FIG. 4. (a) Photon fractions of the polariton modes on the phase-matching ring ($|\mathbf{k}|=k_r$) as a function of the normalized detuning. Upper triangle: upper branch. Lower triangle: lower branch. Thick solid line: the ratio between the lower and upper branch photon fractions. (b) Ring emission external angle θ_r (deg) vs polariton splitting (meV) for different normalized detunings.

luminescence.[22] This coupling is usually described by the quasimode Hamiltonian

$$H_{ext} = \sum_{j,\mathbf{k}} \int d\omega\, g(\omega) |M_{j,2,\mathbf{k}}|^2 \alpha^{\dagger}_{\omega,\mathbf{k}}\, p_{j,\mathbf{k}} + \text{H.c.}, \qquad (11)$$

where $g(\omega)$ is the coupling energy (approximately constant in the mirror spectral stop band) and $\alpha^{\dagger}_{\omega,\mathbf{k}}$ is the creation operator of an extra-cavity photon with energy $\hbar\omega$ and conserved in-plane wave vector $\mathbf{k}$. The free space photon is emitted with an external angle θ with respect to the vertical direction, such as $k=(\omega/c)\sin\theta$. The coupling of each branch ($j \in \{1,2\}$) to the external field is proportional to the photonic fraction $|M_{j,2,\mathbf{k}}|^2$. Importantly, branch-entangled pairs of polaritons can emit frequency-entangled pairs of photons, i.e., states like

$$|\Psi\rangle \propto (\alpha^{\dagger}_{\omega_1,\mathbf{k}_r}\alpha^{\dagger}_{\omega_2,-\mathbf{k}_r} + \alpha^{\dagger}_{\omega_2,\mathbf{k}_r}\alpha^{\dagger}_{\omega_1,-\mathbf{k}_r})|0\rangle, \qquad (12)$$

where $\hbar\omega_1$ ($\hbar\omega_2$) is the energy of the lower (upper) branch state with in-plane wave vector k_r. The frequency entanglement[27] of photon pairs can be measured by coincidence counting in Hong-Ou-Mandel-type interferometers,[28] which are also used in quantum tomography.[4] In order to have a significant extra-cavity visibility, the polariton signal and idler modes need to have a similar coupling to the extra-cavity field. This occurs when the cavity photon fraction of the polariton signal and idler modes is comparable. Figure 4(a) depicts, respectively, the photon fractions $|M_{2,2,k_r}|^2$ and $|M_{1,2,k_r}|^2$ of the upper and lower branch modes on the ring, versus the normalized detuning. The thick solid line shows the ratio $|M_{1,2,k_r}/M_{2,2,k_r}|^2$. Compared to the known intra-branch process[9] where the signal-idler coupling ratio is typically less than 0.05,[21] the interbranch process here described enjoys a higher ratio. At zero detuning, the ratio is $\simeq 0.2$, rising significantly in the region of negative detuning ($\simeq 0.4$ for $\delta=-1$). Finally, Fig. 4(b) shows the dependence of the phase-matching ring wave vector on the polariton coupling. The corresponding emission angle θ_r (deg) increases with increasing polariton splitting. For a given polariton splitting, θ_r depends only on $|\delta|$, being minimum for zero detuning.

D. Losses for the polariton modes

As well known in quantum optics, the interesting quantum regime is achieved when the scattering is spontaneous, i.e., the probability of having more than one entangled pair in the same state is negligible. In other words, the parametric scattering should be kept below the stimulated parametric oscillation threshold.[22,29] However, the system cannot be driven too much below threshold, because other scattering mechanism can prevail, disentangling the pairs created by parametric scattering. Hence, the role of losses is crucial and needs to be carefully addressed.

1. Linear losses

Losses for the polariton modes produce a branch- and wave-vector dependent polariton broadening $\gamma_{j,k}$. In the low excitation regime at low temperatures, the linear broadening $\gamma^L_{j,k}$ is essentially due to the radiative linewidth, the interaction with acoustic phonons,[30] scattering by impurities and, for the upper branch, mixing with the exciton continuum states.[31] The radiative lifetime and the impurity concentration are strongly sample dependent, being determined by the growth quality of the microcavity. Usually, the broadening due to emission of acoustic phonons is smaller with respect to the radiative linewidth and to the impurity-induced losses. On the other hand, the continuum of unbound electron-hole

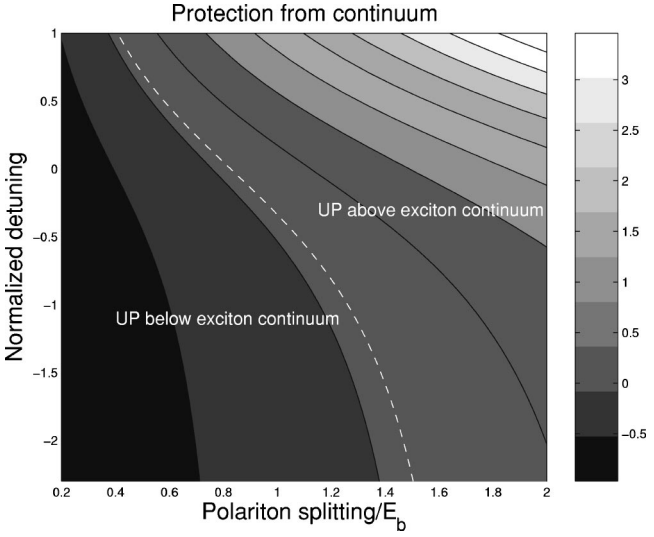

FIG. 5. Contours of $[E_2(k_r)-E_X-E_b]/E_b$ vs $2\hbar\Omega_R/E_b$ and the normalized detuning $\delta=[E_C(0)-E_X]/(2\hbar\Omega_R)$. The white-dashed line depicts the zero value points, i.e., the upper polariton state on the ring is resonant with the continuum band edge. Same parameters as in Fig. 3.

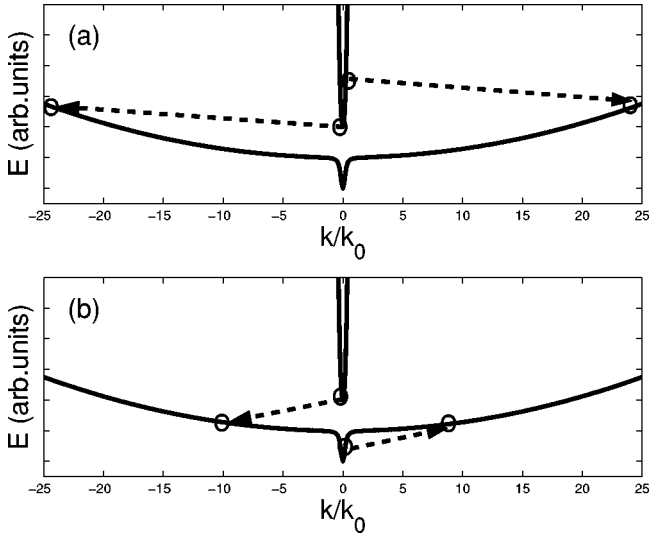

FIG. 6. Sketch of the pair scattering processes responsible for nonlinear losses of the polariton modes. (a) An upper branch polariton scatter with one pump polariton ($k_p=0$) belonging to the upper branch. The final states are excitons with large momentum. (b) Analogous loss process for a lower polariton, due to scattering with one pump polariton.

pairs is a major source of broadening for the upper branch states with energy higher than the continuum onset. In principle, the upper branch state on the ring can form a Fano resonance with the continuum states, with a finite probability of decaying irreversibly into undesirable unbound electron-hole pairs. This issue is addressed in Fig. 5, which shows the difference between the upper branch final-state energy $E_2(k_r)$ and the continuum band edge energy E_X+E_b, in units of E_b. The white-dashed line depicts the points where the difference is 0. The encouraging fact is that there is a wide region with negative values, implying that the upper polariton final-state can be protected from the free carrier absorption. At zero detuning, this occurs for a polariton splitting to exciton binding energy ratio smaller than 0.8. The condition becomes even less stringent for negative detunings.

2. Density-dependent losses

For moderate and higher excitation densities, nonlinear losses[32–36] play an important role. In particular, polariton pair scattering into the exciton reservoir can become the leading source of broadening for the polariton modes. Namely, fast decoherence of the pumped mode can occur due to pump-pump scattering into the high-momentum exciton states, while pump-signal (idler) scattering into the exciton reservoir creates a loss mechanism for the polariton signal (idler) mode. Panel (a) represents the scattering of one upper polariton state with one pump polariton with zero in-plane wavevector. Panel (b) represents the analogous scattering for one lower polariton. Within the Born approximation, the nonlinear broadening is given by

$$\gamma_{j,k}^{NL}=2\pi\sum_{\mathbf{q}}N_{2,\mathbf{0}}|(\lambda_X^2/A)V_{\mathbf{0},\mathbf{k},\mathbf{q}}^{1,1,2,j}|^2\delta(\Delta E), \tag{13}$$

where here δ is the Dirac function, $\Delta E=E_2(0)+E_j(k)-E_1(q)-E_1(|-\mathbf{q}+\mathbf{k}|)$ and $N_{2,\mathbf{0}}$ is the number of polaritons in the pumped mode. If the pump mode is driven coherently (the case of our interest), $N_{2,\mathbf{0}}\simeq|\langle p_{2,\mathbf{0}}\rangle|^2$. Since the energy conservation is fulfilled for a wave vector q very large compared to k (see Fig. 6), we can safely approximate $E_1(|-\mathbf{q}+\mathbf{k}|)\simeq E_1(q)\simeq E_X+(\hbar^2q^2/2M)$, being M the exciton mass. Hence, the expression for the nonlinear broadening becomes

$$\gamma_{j,k}^{NL}\simeq\frac{M\lambda_X^2}{2\hbar^2}|V_{\mathbf{0},\mathbf{k},\overline{q_j}}^{1,1,2,j}|^2(n_{2,\mathbf{0}}\lambda_X^2), \tag{14}$$

where $\overline{q_j}$ is such that $E_2(0)+E_j(k)=2E_1(\overline{q_j})$ and $n_{\mathbf{2,0}}=N_{\mathbf{2,0}}/A$ is the density of pump polaritons per unit area. Let us calculate the nonlinear broadening for a set of realistic parameters, namely, exciton mass $M=0.3\,m_0$, pump density $n_{2,\mathbf{0}}=1/20\,n_{sat}$, polariton splitting $2\hbar\Omega_R=7$ meV, $\lambda_X=10$ nm. For this parameters, we get $\gamma_{1,k_r}^{NL}=1.1$ meV, $\gamma_{2,k_r}^{NL}=0.25$ meV for normalized photon detuning $\delta=+1$. For $\delta=0$, $\gamma_{1,k_r}^{NL}=4.3$ meV, $\gamma_{2,k_r}^{NL}=0.3$ meV, while for $\delta=-0.5$ $\gamma_{1,k_r}^{NL}=6.7$ meV, $\gamma_{2,k_r}^{NL}=0.12$ meV. Note that, under pumping of the upper branch, the collision broadening of the upper polariton state on the ring is smaller than that of the companion state on the lower branch. This occurs because the upper polariton state on the ring has always an excitonic fraction smaller than the lower polariton state with the same wave vector.

E. Collision broadening catastrophe

The spontaneous scattering regime[22] is achieved for pump intensities well below the stimulated parametric oscillation threshold. Since interbranch parametric interaction and pair scattering into the exciton reservoir are due to the same microscopic mechanism, *a priori* it is not clear if a stimulation threshold can be ever achieved under pump excitation of the upper branch. In fact, the parametric oscillation threshold is

achieved when the parametric interaction energy compensates for the total losses of the signal-idler pair, namely,

$$|E^{1,2,2}_{\mathbf{k}_r,0}\ \mathcal{P}^{\rm thr\ 2}_{2,\mathbf{0}}|^2 = (\gamma^L_{1,k_r} + \gamma^{NL}_{1,k_r})(\gamma^L_{2,k_r} + \gamma^{NL}_{2,k_r}), \qquad (15)$$

which is a self-consistent equation, because γ^{NL}_{j,k_r} depends on the pump density. If we define $\xi^{NL}_{j,k} = (M\lambda_X^2/2\hbar^2)|V^{1,1,2,j}_{\mathbf{0},\mathbf{k},q_j}|^2$, then we can rewrite the collision broadening as $\gamma^{NL}_{j,k} = \xi^{NL}_{j,k} n_{2,\mathbf{0}} \lambda_X^2$. Hence, Eq. (15) becomes

$$[(E^{1,2,2}_{\mathbf{k}_r,0})^2 - \xi^{NL}_{1,k_r}\xi^{NL}_{2,k_r}](n^{thr}_{2,\mathbf{0}}\lambda_X^2)^2 = \beta\, n^{thr}_{2,\mathbf{0}}\lambda_X^2 + \gamma^L_{1,k_r}\gamma^L_{2,k_r}, \qquad (16)$$

where $\beta = (\gamma^L_{1,k_r}\xi^{NL}_{2,k_r} + \gamma^L_{2,k_r}\xi^{NL}_{1,k_r})$ is always positive. For typical values of the exciton mass, the quantity $(E^{1,2,2}_{\mathbf{k}_r,0})^2 - \xi^{NL}_{1,k_r}\xi^{NL}_{2,k_r}$ is negative. Hence, Eq. (15) can be never satisfied, because the left-hand side is negative, while the right-hand side is always strictly positive. In other words, the collision broadening due to scattering into the high-momentum states acts as a positive feedback, preventing the system to enter the stimulated regime. This kind of collision catastrophe is absent when the pump excites the lower branch, because the coupling to the high-momentum states is strongly suppressed.[32–36]

II. 1D MICROCAVITIES

The concept of branch entanglement is quite general and can be applied also to multibranch systems, such as photonic wires.[18] In a one-dimensional cavity, the additional confinement along the *y* direction produces a series of cavity photon sub-branches, whose energy dispersion $E_C^{(n_y)}(k_x)$ is given by

$$[E_C^{(n_y)}(k_x)]^2 = [E_C(k_x)]^2 + \frac{(\hbar c)^2}{\epsilon}\left(\frac{\pi(n_y+1)}{L_y}\right)^2, \qquad (17)$$

where $E_C(k_x)$ is the energy of the planar cavity with $k = k_x$, L_y is the wire width and n_y is the sub-branch index (positive or equal to zero). Strong coupling to the exciton resonance produces a many-fold of lower polariton sub-branches with energy $E_1^{(n_y)}(k_x)$ and upper polariton sub-branches with energy $E_2^{(n_y)}(k_x)$. Each cavity sub-band couples to an exciton mode with the same symmetry.[37] The polariton splitting $2\hbar\Omega_R$ is approximately independent[37] of the branch index n_y for small values of n_y. As experimentally demonstrated in the experiments by Dasbach *et al.*[18], there are many new parametric scattering channels available. In particular, it is possible to have inter-branch scattering by pumping one lower sub-branch.[18] The momentum conservation along the *y* direction is lifted, being replaced by the less stringent *parity* selection rule.[18,38] This selection rule for pair scattering of 1D polaritons imposes that the sum of n_y for signal and idler must be even. The interbranch parametric scattering process has an efficiency,[39] which is comparable to the intrabranch scattering in planar microcavities. In Fig. 7, we propose a scattering process, in which the pump excites the lower sub-branch with $n_y = 2$ and $k_x = 0$. For a proper exciton-photon detuning, there is a phase-matched process, in which the final states are two polariton modes with opposite and finite wave vectors, one belonging to the lower $n_y = 0$ sub-branch and the other to the upper $n_y = 0$ sub-branch. The phase-matching function for this interbranch scattering channel is depicted in Fig. 8, as a function of the wave vector k_x and the normalized detuning $\Delta = [E_C(0) - E_X]/(2\hbar\Omega)$, where $E_C(0)$ is the 2D-cavity energy and $2\hbar\Omega_R$ is the polariton splitting. As in Fig. 2, the phase-matching function is equal to 2, when there are two branch-exchanged processes, which are exactly phase-matched (the condition for branch entanglement). For zero pump wave vector k_p [see Fig. 8(a)], this property is achieved in a broad, but finite range of negative detuning Δ. In contrast to the 2D case, for $k_p \neq 0$, the phase-matching function is equal to 2 only at the pump wave vector, as shown in Fig. 8(b). But this does not correspond to pure polariton branch-entanglement, because signal and idler have the same wave-vector.

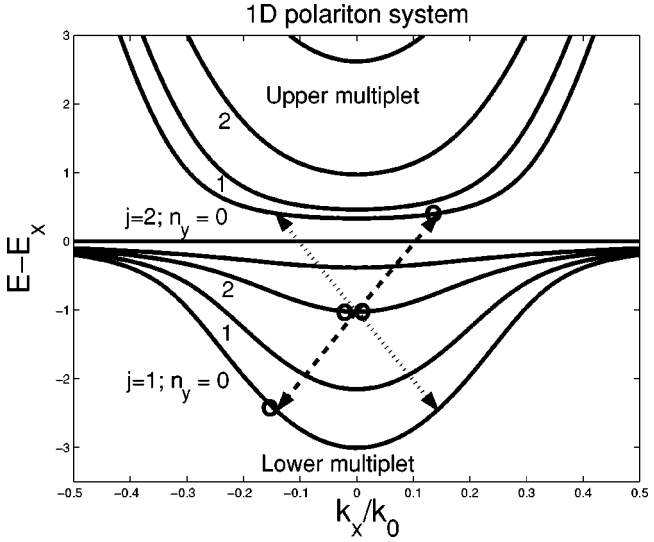

FIG. 7. Energy dispersion (units of $2\hbar\Omega_R$) of 1D polaritons as a function on the wave vector k_x (k_0 units) along the direction of the photonic wire. Compared to the 2D system, the lower branch ($j=1$) is split in a multiplet of sub-branches ($n_y = 0, 1, 2, \ldots$), as well as the upper branch ($j=2$). The arrows depict the considered inter-branch parametric scattering process, in which the pump excites the $n_y = 2$ lower sub-branch mode with $k_x = 0$. Parameters: $2\hbar\Omega_R = 4$ meV, wire width $L_y = 4\ \mu$m, $E_X = E_C(0) + 4\hbar\Omega_R$, with $E_C(0) = 1.5\ e$V is the 2D-cavity energy.

Importantly, in a photonic wire it is possible to have inter-sub-branch scattering processes restricted to the lower many-fold only. One parity-conserving process is shown in Fig. 9, where the pump excites the $n_y = 2$ sub-branch at $k_x = 0$ and the signal and idler modes belong to the $n_y = 1$ and $n_y = 3$ sub-branches. The phase-matching properties of this processes are reported in Fig. 10 as a function of the signal wave vector along the wire direction and of the normalized detuning Δ.

The interest of photonic wires does not rely only in the possibility of having new scattering channels. One advantage is to provide a much better protection from the exciton reservoir. In fact, in contrast to pumping of the upper branch, the interbranch process shown in Fig. 7 suffers much weaker nonlinear losses due to pair scattering into the high-momentum exciton states. As already studied theoretically and experimentally, under excitation of the lower branch,

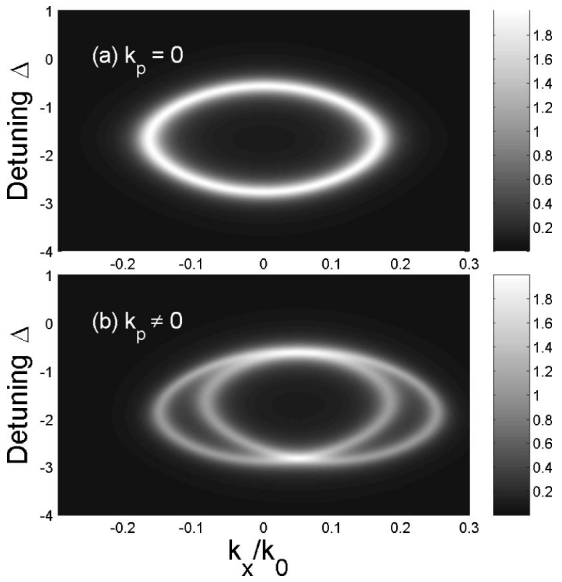

FIG. 8. Phase-matching function for the inter-sub-branch scattering of 1D polaritons depicted in Fig. 7, as a function of k_x (k_0 units) and the normalized detuning $\Delta=(E_C(0)-E_X)/(2\hbar\Omega)$, with $E_C(0)$ the 2D-cavity energy. (a) $\mathbf{k}_p=\mathbf{0}$. (b) $\mathbf{k}_p=0.05\ k_0\hat{\mathbf{x}}$. Parameters: $2\hbar\Omega_R=4$ meV, $\gamma=0.5$ meV.

pump-pump scattering into the exciton reservoir is strongly suppressed due to lack of energy-momentum conservation.[33,34,36] The same is true for pump-signal and pump-idler scattering. The only allowed channel is the signal-signal (or idler-idler) scattering, in which the signal (idler) mode belong to the upper branch. But this is not a crucial process especially below or near threshold, when the signal (idler) population is much smaller than the pump one.

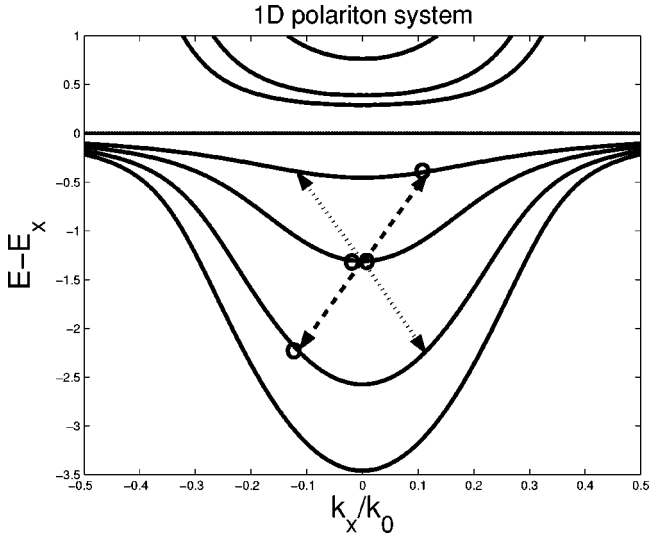

FIG. 9. Arrows depict the inter-sub-branch scattering, with all states belonging to the lower many-fold. Parameters: $2\hbar\Omega_R=4$ meV, wire width $L_y=4$ μm, $E_X=E_C(0)+3.5\ \hbar\Omega_R$, with $E_C(0)=1.5$ eV is the 2D-cavity energy. Horizontal and vertical axis as in Fig. 7.

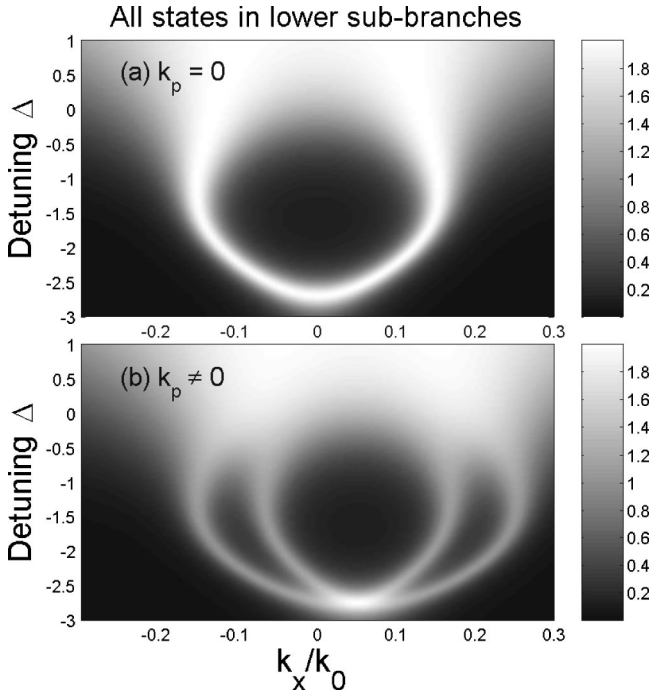

FIG. 10. Phase-matching function for the inter-subbranch scattering of 1D polaritons depicted in Fig. 9, as a function of k_x (k_0 units) and the normalized detuning $\Delta=[E_C(0)-E_X]/(2\hbar\Omega)$, with $E_C(0)$ the 2D-cavity energy. (a) $\mathbf{k}_p=\mathbf{0}$. (b) $\mathbf{k}_p=0.05\ k_0\hat{\mathbf{x}}$. Parameters: $2\hbar\Omega_R=4$ meV, $\gamma=0.4$ meV.

III. CONCLUSIONS

In conclusion, we have proposed and analyzed a scheme for the generation of branch-entangled polariton pairs in semiconductor microcavities through spontaneous inter-branch parametric scattering. Branch entanglement of polariton pairs leads to emission of frequency-entangled pairs of extra-cavity photons, which have been recently attracting considerable attention in the field of quantum tomography.[4] This kind of nonclassical states cannot be achieved by intra-branch polariton pair scattering,[9] being a peculiarity of inter-branch processes. In planar microcavities, the phase-matching conditions are satisfied by pumping the upper polariton branch for an arbitrary pump in-plane wave vector $\mathbf{k}_p$. We have studied the phase-matching properties and the efficiency of the process as a function of exciton-photon detuning, polariton splitting and exciton binding energy. While the phase-matching properties for the 2D interbranch process are very flexible, the nonlinear losses due to polariton pair scattering into the high-momentum exciton states is a reason of concern, being a significant source of decoherence. The lack of protection of pump polaritons in the upper branch can be naturally overcome in photonic wires, thanks to the existence of a many-fold of sub-branches. In this paper, we have shown that there are parity-conserving interbranch scattering processes (forbidden in planar microcavities), in which the pump excites a lower polariton sub-branch mode with $k_x=0$, providing branch entanglement of the signal-idler polariton pair. These processes enjoy much better protection from the high-momentum exciton states, making one-dimensional mi-

crocavities a strong candidate to demonstrate and exploit the quantum effects here proposed. Current experiments in photonic wires are encouraging.[40] In the future, we would like to address interesting features such as the dynamics of entanglement generation. We hope that the ideas presented in this paper will stimulate experimental and theoretical research in a field at the frontier between condensed matter physics and quantum optics. Indeed, one challenging, but intriguing goal would be the development of polariton micro-sources of non-classical states with controllable properties.

ACKNOWLEDGMENTS

We wish to thank J. Tignon, G. Bastard, G. Dasbach, Ph. Roussignol, and M. Saba for discussions. LPA-ENS (former LPMC-ENS) is "Unité Mixte de Recherche Associé au CNRS (UMR 8551) et aux Universités Paris 6 et 7."

[1] J. M. Raimond, M. Brune, and S. Haroche, Rev. Mod. Phys. **73**, 565 (2001).

[2] P. G. Kwiat, K. Mattle, H. Weinfurter, A. Zeilinger, A. V. Sergienko, and Y. Shih, Phys. Rev. Lett. **75**, 4337 (1995).

[3] N. Gisin, G. Ribordy, W. Tittel, and H. Zbinden, Rev. Mod. Phys. **74**, 145 (2002).

[4] M. B. Nasr, B. E. A. Saleh, A. V. Sergienko, and M. C. Teich, Phys. Rev. Lett. **91**, 083601 (2003).

[5] H. Pu and P. Meystre, Phys. Rev. Lett. **85**, 3987 (2000).

[6] C. Weisbuch, M. Nishioka, A. Ishikawa, and Y. Arakawa, Phys. Rev. Lett. **69**, 3314 (1992).

[7] R. Houdré, C. Weisbuch, R. P. Stanley, U. Oesterle, P. Pellandini, and M. Ilegems, Phys. Rev. Lett. **73**, 2043 (1994).

[8] For a recent review, see Semicond. Sci. Technol. **18**, S279 (2003), *special issue on semiconductor microcavities*, edited by J. J. Baumberg and L. Vinã.

[9] P. G. Savvidis, J. J. Baumberg, R. M. Stevenson, M. S. Skolnick, D. M. Whittaker, and J. S. Roberts, Phys. Rev. Lett. **84**, 1547 (2000).

[10] P. G. Savvidis, J. J. Baumberg, R. M. Stevenson, M. S. Skolnick, D. M. Whittaker, and J. S. Roberts, Phys. Rev. B **62**, R13278 (2000).

[11] R. M. Stevenson, V. N. Astratov, M. S. Skolnick, D. M. Whittaker, M. Emam-Ismail, A. I. Tartakovskii, P. G. Savvidis, J. J. Baumberg, and J. S. Roberts, Phys. Rev. Lett. **85**, 3680 (2000).

[12] J. J. Baumberg, P. G. Savvidis, R. M. Stevenson, A. I. Tartakovskii, M. S. Skolnick, D. M. Whittaker, and J. S. Roberts, Phys. Rev. B **62**, R16247 (2000).

[13] G. Messin, J. Ph. Karr, A. Baas, G. Khitrova, R. Houdré, R. P. Stanley, U. Oesterle, and E. Giacobino, Phys. Rev. Lett. **87**, 127403 (2001).

[14] M. Saba, C. Ciuti, J. Bloch, V. Thierry-Mieg, R. André, Le Si Dang, S. Kundermann, A. Mura, G. Bongiovanni, J. L. Staehli, and B. Deveaud, Nature (London) **414**, 731 (2001).

[15] A. Huynh, J. Tignon, O. Larsson, Ph. Roussignol, C. Delalande, R. André, R. Romestain, and Le Si Dang, Phys. Rev. Lett. **90**, 106401 (2003).

[16] S. Kundermann, M. Saba, C. Ciuti, T. Guillet, U. Oesterle, J. L. Staehli, and B. Deveaud, Phys. Rev. Lett. **91**, 107402 (2003).

[17] G. Dasbach, M. Schwab, M. Bayer, and A. Forchel, Phys. Rev. B **64**, 201309 (2001).

[18] G. Dasbach, M. Schwab, M. Bayer, D. N. Krizhanovskii, and A. Forchel, Phys. Rev. B **66**, 201201 (2002).

[19] P. Schwendimann, C. Ciuti, and A. Quattropani, Phys. Rev. B **68**, 165324 (2003).

[20] J. Ph. Karr, A. Baas, R. Houdré, and Elisabeth Giacobino, Phys. Rev. A **69**, 031802 (2004).

[21] J. Ph. Karr, A. Baas, and E. Giacobino, cond-mat/0306236 (unpublished).

[22] C. Ciuti, P. Schwendimann, and A. Quattropani, Phys. Rev. B **63**, 041303 (2001).

[23] W. Langbein, in *Proceedings of the Twenty Sixth International Conference on the Physics of Semiconductors* (IOP, Edinburgh, UK, 2002).

[24] F. Tassone, and Y. Yamamoto, Phys. Rev. B **59**, 10 830 (1999).

[25] C. Ciuti, P. Schwendimann, B. Deveaud, and A. Quattropani, Phys. Rev. B **62**, R4825 (2000).

[26] For a review of quantum optical properties of entangled photons, see, e.g., Y. Shi, Rep. Prog. Phys. **66**, 1009 (2003).

[27] The emission angles corresponding to ω_1 and ω_2 are slightly different $[\Delta\theta_r/\theta_r \simeq (\omega_2-\omega_1)/\omega_1$, typically less than 1%] . Hence, the emitted photon pair is also momentum entangled.

[28] C. K. Hong, Z. Y. Ou, and L. Mandel, Phys. Rev. Lett. **59**, 2044 (1987); H. Kim, J. Ko, and T. Kim, Phys. Rev. A **67**, 054102 (2003).

[29] D. M. Whittaker, Phys. Rev. B **63**, 193305 (2001).

[30] F. Tassone, C. Piermarocchi, V. Savona, A. Quattropani, and P. Schwendimann, Phys. Rev. B **56**, 7554 (1997).

[31] D. S. Citrin and J. B. Khurgin, Phys. Rev. B **68**, 205325 (2003).

[32] J. J. Baumberg, A. Armitage, M. S. Skolnick, and J. S. Roberts, Phys. Rev. Lett. **81**, 661 (1998).

[33] C. Ciuti, V. Savona, C. Piermarocchi, A. Quattropani, and P. Schwendimann, Phys. Rev. B **58**, R10123 (1998).

[34] T. Baars, M. Bayer, A. Forchel, F. Schäfer, and J. P. Reithmaier, Phys. Rev. B **61**, R2409 (2000).

[35] S. Savasta, O. Di Stefano, and R. Girlanda, Phys. Rev. Lett. **90**, 096403 (2003).

[36] A. Huynh, J. Tignon, G. Keller, Ph. Roussignol, C. Delalande, R. André, R. Romestain, and Le Si Dang, Phys. Rev. B **68**, 165340 (2003).

[37] A. I. Tartakovskii, V. D. Kulakovskii, A. Forchel, and J. P. Reithmaier, Phys. Rev. B **57**, R6807 (1998).

[38] G. Dasbach, Ph.D. thesis, University of Dortmund, 2003.

[39] L. M. Woods and T. L. Reinecke, Phys. Rev. B **67**, 115336 (2003).

[40] G. Dasbach and J. Tignon (private communication).